# Salt-Induced Vesicle to Micelle Transition in Aqueous Solution of Sodium *N*-(4-*n*-Octyloxybenzoyl)-L-valinate

**Ashok Mohanty,† Trilochan Patra, and Joykrishna Dey***

*Department of Chemistry, Indian Institute of Technology, Kharagpur − 721 302, India*

*Received: February 15, 2007; In Final Form: April 30, 2007*

The self-organization of a single-tailed amino acid based chiral surfactant sodium *N*-(4-*n*-octyloxybenzoyl)-L-valinate (SOBV) has been studied in water. A number of techniques like surface tension, fluorescence probe, dynamic light scattering (DLS), transmission electron microscopy (TEM), and atomic force microscopy (AFM) have been utilized for characterization of the self-assemblies. The amphiphile forms large spherical vesicles of 400−600 nm diameters in dilute aqueous solution. However, the vesicles get transformed into spherical micelles with increase of surfactant concentration or upon addition of relatively low amount (20 mM) of NaCl or KCl. This is the first example of salt-induced vesicle to micelle transition (VMT) in a single surfactant system. The vesicles are stable in the temperature range of 30−70 °C. Cleavage of intermolecular hydrogen bonds among the amide groups in the presence of salt appears to be the plausible cause for the VMT.

## Introduction

Amphiphilic molecules have a tendency to form organized assemblies of different shape and size in solutions above a threshold concentration called critical aggregation concentration (*cac*).[1] The morphology of the self-assemblies formed (spherical and non spherical micelles, vesicles, and lyotropic liquid crystalline structures) primarily depends on the molecular structure of the amphiphile.[1] The environmental factors like surfactant concentration, temperature, pH, and ionic strength have also a profound effect on the aggregate formation.[2] In fact, it is possible to get transformation from one type of aggregates to other by changing these environmental factors.[3] In this regard, the vesicle to micelle transition (VMT) has gained considerable attention in recent years because of its fundamental importance and potential applications.[4−8] The majority of VMT reported so far is in catanionic surfactant systems.[5−8] The VMT is achieved by varying temperature,[5] addition of co-surfactants,[6] or by application of external forces like shear.[7] More recently, pH induced VMT has been reported in case of a sugar based gemini surfactant system.[8] In all these cases, authors have achieved transition from vesicles to either cylindrical, threadlike, or wormlike micelles. However, in the literature, report of salt-induced VMT is rare. This is because addition of salt is known to favor formation of lager aggregates by reducing the electrostatic repulsion among the headgroups and thus favoring tight packing of the surfactant monomers in the aggregates.[9] In fact, there are reports of salt induced vesicle formation in some surfactant systems.[10] In a recent report, Lu and co-workers[11] in their study involving a catanionic system consisting of a cationic bola amphiphile and anionic sodium n-dodecyl sulfate have reported that addition of low concentrations of salt favors transformation of vesicles to tubules, but the vesicles get transformed to spherical micelles at high salt concentrations (0.1 M).

During our ongoing effort of developing new chiral surfactants that are used as chiral selectors for enantiomeric separations using capillary electrophoresis (CE),[12] we observed that the L-amino acid based amphiphile sodium *N*-(4-*n*-octyloxybenzoyl)-L-valinate (SOBV, see Figure 1 for molecular structure) forms micelles[13] in borate buffer pH 9.7 contrast to sodium *N*-(4-*n*-dodecyloxybenzoyl)-L-valinate (SDBV), which forms vesicles.[12a,b] Nevertheless, SOBV was successfully used as a chiral selector for enantiomeric separations of some selected chiral organic molecules.[13] The formation of different types of self-assemblies (micelles and vesicles) by the structurally similar SOBV and SDBV in borate buffer pH 9.7 led us to study in detail the aggregation behavior of SOBV in water. As will be discussed later, it was observed that SOBV spontaneously formed spherical vesicles like SDBV[14] in pure water. However, unlike SDBV, the vesicles of SOBV get completely transformed into spherical micelles at higher surfactant concentrations or with addition of relatively low amount (20 mM) of NaCl or KCl. Based on the results of $^1$H NMR and fluorescence probe studies, a plausible mechanism for the VMT is proposed.

## Experimental Section

**Materials.** The surfactant SOBV was synthesized and purified in the laboratory following the reported procedure.[12,14] The fluorescence probes *N*-phenyl-L-naphthylamine (NPN), and 1,6-diphenyl-1,3,5-hexatriene (DPH) were purchased from Sigma-Aldrich and were recrystallized twice from an ethanol-acetone mixture prior to use. The purity of the compounds was checked by measuring the fluorescence excitation and emission spectra at several wavelengths. Uranyl acetate was purchased from Aldrich and was directly used from the bottle. Analytical grade sodium chloride, and other organic solvents were procured locally from SRL, Mumbai, India.

**General Instrumentation.** NMR spectra were recorded using a Bruker SEM 200 instrument in $CDCl_3$ solvent using trimethylsilane (TMS) as the internal standard. UV−vis spectra were recorded on a Shimadzu model 1601 spectrophotometer. The pH measurements were done with a digital pH meter, model

* Author for correspondence; Telephone: 91-3222-283308, Fax: 91-3222-255303. E-mail: joydey@chem.iitkgp.ernet.in.

† Present address: Analytical Chemistry Centre, National Metallurgical Laboratory, Jamshedpur, India.

10.1021/jp071312s CCC: $37.00 
Published on Web 06/07/2007

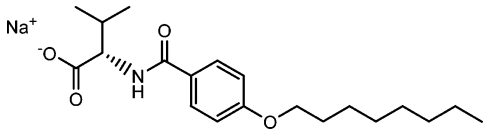


**SOBV**

**Figure 1.** Molecular structure of sodium *N*-(4-n-octyloxybenzoyl)-L-valinate (SOBV).

pH 5652 (EC India Ltd., Calcutta), using a glass electrode. Distilled water was deionized (resistivity 18.2 MΩ) using a Milli-Q water purification system (Millipore, USA).

**Surface Tension Measurements.** Surface tension measurements were performed using a torsion balance (S.D. Hurdson & Co., Calcutta) using the Du Nüoy ring detachment method. A stock solution of the surfactant was prepared using deionized water (pH 6.8). An aliquot of the stock solution was added to a beaker containing a known volume of water. The solution was stirred gently using a magnetic stirrer, and the surface tension was measured after equilibration for 5 min at room temperature (30 °C). Three measurements were performed for each sample, and the mean $\gamma$ (mN m$^{-1}$) value was recorded. The *cac* was then obtained from the break point of the plot of $\gamma$ versus log C.

**Fluorescence Measurements.** Steady-state fluorescence experiments were carried out with a Perkin-Elmer LS-55 luminescence spectrometer equipped with a filter polarizer and a thermostated cell holder. Temperature was controlled using a circulating bath (Thermo Neslab, RTE 7). For solution preparations, a saturated solution of NPN in deionized water (pH 6.8) was used. DPH concentration was kept at $1 \times 10^{-6}$ M. NPN was excited at 340 nm, and emission spectra were recorded in the wavelength range of 360−600 nm. For fluorescence anisotropy measurements in the presence of surfactant vesicles, DPH was excited at 350 nm and the fluorescence intensity was measured at 450 nm. To reduce the effect of scattered light, if any, a 430 nm cutoff filter was placed in the emission beam. The excitation and emission slit widths were 2.5 and 5 nm, respectively. The fluorescence measurements were performed at 30 °C if not mentioned otherwise.

**Light-Scattering Measurements.** A Zetasizer Nano ZS light scattering apparatus (Malvern Instruments, U.K.) with a He−Ne laser (633 nm, 4 mW) was used for DLS measurements. The Nano ZS instrument incorporates noninvasive backscatter (NIBS) optics with a detection angle of 173°. The *z*-average diameter and the PDI of the samples were automatically provided by the instrument using cumulant analysis. The size quoted throughout this paper is the *z*-average diameter. For particle size measurements, a surfactant solution of appropriate concentration was made in Milli-Q water (pH 6.8) and was filtered directly into the quartz cell using a Millex-GV (Millipore) membrane filter (0.45 $\mu$m pore size). The quartz cell was rinsed several times with filtered water and then filled with the filtered sample solution. The DLS measurements began 5−10 min after the sample cell was placed in the DLS optical system. The data obtained in each case are the average of 50 runs, each run of 10 s duration. The temperature was maintained at 30 °C.

**Transmission Electron Microscopy.** A Philips CM 200 electron microscope operating at a voltage of 120 kV was used for TEM measurements. The surfactant solutions were filtered through a Millex-GV (Millipore) membrane filter of 0.45 $\mu$m pore size. A drop of the surfactant solution was placed on the carbon-coated copper grid and was allowed to stand for 2 min. The excess solution was blotted off with filter paper followed by staining with 2% aqueous uranyl acetate solution (pH 7.5 or 8.0). The specimens were then dried in a desiccator until before the measurement.

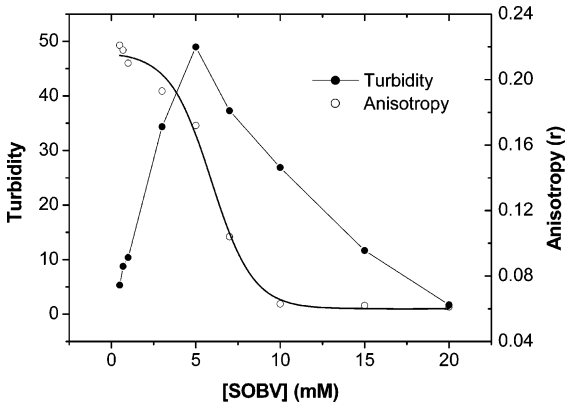


**Figure 2.** Variation of solution turbidity and fluorescence anisotropy (*r*) of DPH at different SOBV concentrations in water.

**Atomic Force Microscopy.** AFM imaging was carried out on a Solver P47-PRO atomic force microscope (NT−MDT, Russia) with contact mode. In order to prepare the samples, a small drop of the vesicle solution (5 mM) was placed on a thin rectangular glass cover slip of 50 mm × 50 mm dimension and was air-dried. The cover slip was then gently placed on the double-sided adhesive tape previously mounted on the metal stubs provided by the instrument manufacturer, which in turn was placed in the sample stage of the microscope. A 10 $\mu$m × 10 $\mu$m scanner and cantilevers with integrated pyramidal silicon probes with a spring constant of 50 N/m was used for the imaging. A suitable area in the sample was located using a video camera mounted above the AFM. After selecting the proper area, imaging was performed choosing a scan area of 5 $\mu$m × 5 $\mu$m.

## Results and Discussion

First, the critical aggregation concentration (*cac*) of SOBV was determined in pure water by surface tension measurement method. The *cac* was measured to be $5.4 \times 10^{-4}$ M, which is around twenty times higher than the *cac* of SDBV.[13] This is not surprising considering the short hydrophobic tail in SOBV compared to SDBV. The *cac* was further determined by fluorescence probe studies using NPN as the probe molecule following the reported procedure[15] (see Supporting Information). The *cac* ($5.6 \times 10^{-4}$ M) thus obtained is closely similar to the value obtained using surface tension measurement and thus confirms the accuracy of the *cac* value. The small difference in the *cac* values obtained by the two methods might be due to turbidity of the solutions at concentrations just above *cac*. The cloudiness of the aqueous SOBV solution above *cac* initially increases with increase of SOBV concentration, reaches a maximum, and then disappears after reaching a certain concentration. The process was followed spectrophotometrically by measuring turbidity, $\tau$ (=100 % T) of the surfactant solutions of different concentrations at 600 nm, where the surfactant has no absorbance (Figure 2). The maximum turbidity was observed at around 5 mM and the solution became clear after 20 mM. This observation suggests some type of transition from bigger to smaller aggregates with the increase of SOBV concentration. It may be noted here that the pH of the solution varies from 7.5 to 8.0 in the surfactant concentration range studied (1−20 mM). The transition was further indicated by steady-state fluorescence anisotropy study.

In order to find the nature of the aggregates formed, we measured fluorescence anisotropy (*r*) of DPH in presence of

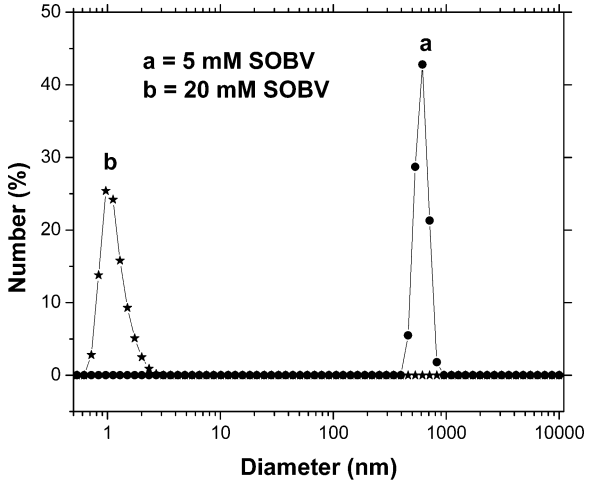


**Figure 3.** Size distribution profile of aggregates in 5 mM and 20 mM SOBV in water.

different concentrations (>*cac*) of SOBV in water. DPH is a widely used probe to study both the static and dynamic properties of membranes, such as membrane fluidity and ordering of lipid acyl chains.[16] Normally, higher values of *r* indicate formation of bilayer aggregates. On the other hand, lower values of *r* correspond to micellar structures.[16] At SOBV concentrations just above *cac* value, the *r*-value is higher (∼0.20) which decreases with the increase of SOBV concentration (Figure 2). The sigmoid nature of the curve suggests transition of the aggregates from a highly ordered state to a less ordered state.[15,16] It should be noted here that the viscosity of the surfactant solution does not change significantly at higher SOBV concentrations eliminating the possibility of formation of wormlike micelles.[5a,17] The inflection point of the graph resembles closely with the point of highest turbidity.

To further investigate the transition process, dynamic light scattering measurements were carried out to measure the size of the aggregates at two different SOBV concentrations of 5 mM (having highest turbidity and high *r* value) and 20 mM (of lowest turbidity and low *r* value). The size distribution profile of the aggregates is shown in Figure 3. The distribution profile is monomodal with relatively low PDI values (0.136 and 0.197 for 5 mM and 20 mM, respectively) suggesting the existence of spherical aggregates of uniform size in both the solutions. The Z-average hydrodynamic diameter ($D_h$) of the aggregates obtained by cumulant analysis was 620 and 2 nm for 5 mM and 20 mM SOBV solution, respectively. The monomodal size distribution with low PDI and higher $D_h$ values exclude the possibility of formation of bilayer lamellar and tubular structures at higher surfactant concentrations. On the other hand, the monomodal size distribution with low PDI and very low $D_h$ value eliminate the possibility of formation of rod-like micelles as a result of fusion of vesicles as reported for other surfactants in the literature.[14,15] Thus the DLS results along with the turbidity and fluorescence anisotropy studies suggest formation of spherical vesicles at lower SOBV concentrations and spherical micelles at higher SOBV concentrations.

To further visualize the microstructure of the self-assemblies, TEM and AFM techniques were utilized. Both TEM and AFM micrographs (Figure 4) show the existence of spherical vesicles in 5 mM SOBV solutions. The vesicle diameters (400−600 nm) as seen in the micrographs are in close agreement with the DLS results. The wall thickness of the vesicles suggests that they are multilamellar type. However, no recognizable structure was observed when the specimens made from 20 mM SOBV

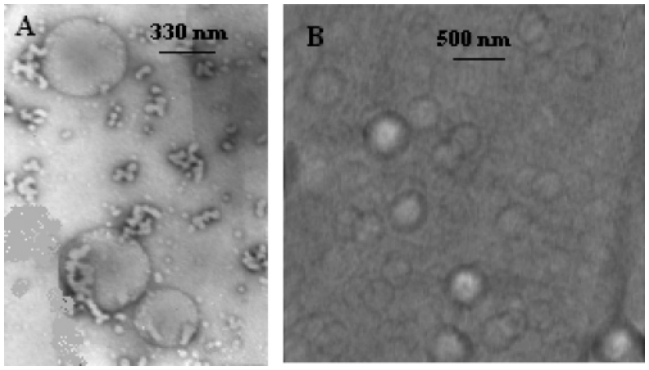


**Figure 4.** TEM (A) and AFM (B) micrographs of 5 mM SOBV in water.

solution was viewed under the TEM microscope. This is perhaps due to the very small size of the aggregates formed in concentrated solutions and is consistent with the results of DLS studies. The microscopic investigations thus confirm existence of large multilamellar vesicles and small micelles, respectively, in dilute and concentrated solutions of SOBV.

It has been reported earlier by our research group[15,18,19b] as well as by others[20] that in the case of carboxylate surfactants, the vesicle formation is more favored at pH around their p$K_a$ values (∼5). Since both carboxylate (−$COO^-$) and protonated (−COOH) forms of the surfactant are present at this pH region, the headgroups of adjacent surfactant molecules can approach closer facilitating formation of intermolecular hydrogen bonds between −$COO^-$ and −COOH groups. This brings hydrocarbon chains closer to each other thereby facilitating intermolecular hydrogen bond formation between amide groups. In order to demonstrate amide−amide hydrogen bond formation, $^1$H NMR spectra of *N*-(4-*n*-octyloxybenzoyl)-L-valine were recorded in $CDCl_3$ at two different concentrations (see Supporting Information). The spectra show a shift of the peak corresponding to CON*H* proton from 6.52 ppm in 5 mM to 6.68 ppm in 150 mM SOBV solution. Although the amide−water hydrogen bonding is a competing factor during aggregation in aqueous solution, the expulsion of water molecules from the vesicle bilayer region after aggregate formation favors the amide−amide hydrogen bonding and contributes toward the stability of the vesicles. The hydrogen bonding interactions and $\pi-\pi$ stacking of the benzene rings result in formation of bilayer structures.[15] The role of hydrogen bonding interactions on vesicle formation is also reported for other surfactants.[19]

The surfactant molecule being sodium salt of a weak acid, get hydrolyzed in water according to the reaction

$$RCOO^-Na^+ + H_2O = RCOOH + Na^+ + OH^- \quad (1)$$

This is indicated by the pH (=7.5) in dilute (5 mM) surfactant solution. With the increase of surfactant concentration, the equilibrium is shifted more toward right resulting in an increase of pH to 8.0. It should be noted here that the p$K_a$ of this class of carboxylic acids solubilized in the vesicle is about 7.0.[15,19b] Since one unit pH increase (from 7.0 to 8.0) around p$K_a$, which occurs due to increase of surfactant concentration to 20 mM causes a large increase in ionization, most of the solubilized carboxylic acid form of the surfactant molecule become ionized. This results in enhanced electrostatic repulsion between surfactant headgroups and thus triggers rupture of the amide−amide hydrogen bond. The result is a complete disruption of the bilayer structure and increase of membrane fluidity as manifested by the decrease of fluorescence anisotropy of DPH probe (Figure

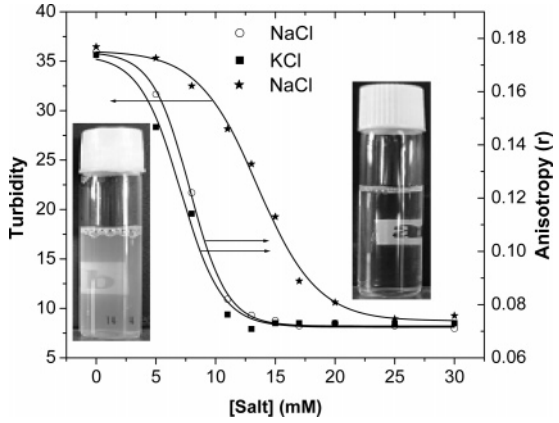


**Figure 5.** Effect of [NaCl] and [KCl] on turbidity and fluorescence anisotropy of DPH in 5 mM aqueous SOBV. Inset: photograph of vials containing 5 mM SOBV solution in water (a) with and (b) without addition of 20 mM NaCl. The visibility of the letter (**a** or **b**) put at the back of the respective vials shows turbidity and transparency of the solutions.

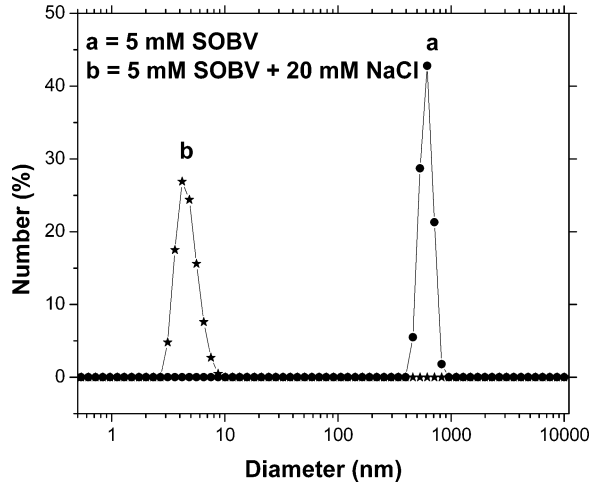


**Figure 6.** Size distribution profile of the aggregates of 5 mM SOBV in water in presence and absence of 20 mM NaCl.

2). That is the VMT that occurs at higher surfactant concentration is induced by the increase of pH.

The effect of salt concentration on the aggregation behavior was then investigated. It was observed that the initial cloudiness of the 5 mM SOBV solution disappeared with time upon addition of NaCl or KCl. The turbidity undergoes a sigmoid decrease with the increase of both NaCl and KCl concentration. The plots in Figure 5 show that the solution becomes clear when 20 mM NaCl is added. The decrease of turbidity is also accompanied by a decrease of fluorescence anisotropy of DPH probe (Figure 5) with the increase of both NaCl and KCl concentration. This could be attributed to salt-induced VMT. This is supported by the results of DLS studies. It was observed that the Z-average hydrodynamic diameter of the aggregates in 5 mM SOBV solution in pure water decreased from 620 to 4 nm with the addition of 20 mM salt. The size distribution profiles of the aggregates in both the cases are shown in Figure 6.

To further strengthen our claim of salt-induced VMT, we have performed an experiment, which suggests the release of trapped molecules in the aqueous cavity of the vesicles when they are transformed into micelles due to addition of salt. The vesicle solution was prepared by dissolving 5 mM amount of solid SOBV in saturated aqueous NPN solution. The fluorescence emission spectrum of NPN was then recorded before and after

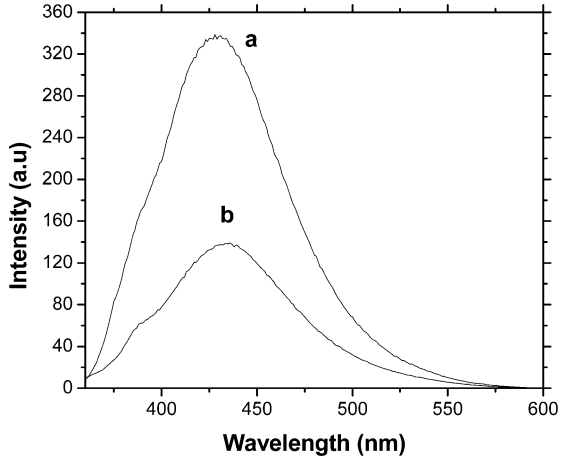


**Figure 7.** Fluorescence emission spectra of NPN in 5 mM SOBV solution in (a) presence and (b) absence of 20 mM NaCl.

addition of 20 mM NaCl to the solution. The increase in fluorescence intensity of NPN emission spectrum (Figure 7) after addition of NaCl suggests the release of NPN trapped in the vesicle aqueous cavity. It is interesting to note that the SOBV vesicles are stable in the temperature range of 30−70 °C. This was indicated by both fluorescence anisotropy and DLS studies. The *r*-value and the Z-average size of the vesicles do not change appreciably in this temperature range (see Supporting Information).

The salt-induced transformation of vesicles to rod-like micelles in aqueous solution of the sodium salts of some *N*-acyl peptides has been recently reported from this laboratory.[18] A plausible explanation of the salt-induced VMT observed in the case of SOBV is probably the weakening of intermolecular hydrogen bonding interactions among the $-COOH$ and $-COO^-$ groups in the presence of salt. As explained earlier this triggers disruption of the bilayer structure. However, as noted earlier, the vesicles of structurally similar SDBV surfactant remain unchanged upon addition of NaCl. The insensitiveness of SDBV vesicles to NaCl addition might be due to stronger hydrophobic interaction between hydrocarbon chains relative to that in SOBV molecule the hydrocarbon chain length of which is shorter than that of the former. This is manifested by the higher *cac* value in the case of SOBV surfactant. Initially we thought that the salt-induced VMT might be a consequence of the change of solution pH. However, it was observed that the pH (=7.5) of the starting solution increased only by ∼0.3 unit upon addition of 20 mM NaCl or KCl. To further examine the effect of pH we also measured fluorescence anisotropy of DPH probe in the presence of 5 mM SOBV in 20 mM phosphate buffer (pH = 7.3, $I = 0.05$). The *r*-value (0.07) was found to be much lower than that in pure water (∼0.2). This suggests that the decrease in turbidity or *r*-value upon addition of NaCl or KCl is due only to the salt effect but not caused by the small increase of pH. The weakening of hydrogen bonds in the presence of salts is also reported by many authors.[21] Berkowitz and co-workers[22] have also reported cleavage of hydrogen bond between $-COO^-$ and $NH_3^+$ groups in dipalmitoylphosphatidylserine bilayer in the presence of NaCl due to binding of $Na^+$ counterion with the $-COO^-$ group of serine. Similar mechanism might be involved in the disruption of the bilayer vesicles of SOBV surfactant. Binding of $Na^+$ or $K^+$ counterion with the $-COO^-$ group may lead to the cleavage of the hydrogen bond between adjacent $-COOH$ and $-COO^-$ groups and thus triggers the breakdown of the vesicle structure as explained earlier for pH-induced VMT.

## Conclusion

In summary, salt-induced transition from spherical vesicles to spherical micelles is demonstrated for the first time for a simple anionic surfactant system. The vesicles get transformed into micelles in the presence of 20 mM NaCl. The VMT could be followed visually by monitoring the turbidity of the solution with naked eye. Although, in a recent publication,[18] one of us speculated such transition of vesicle to rod-like micelles in the cases of some *N*-acyl peptide surfactants, to the best of our knowledge, this is the first report of salt-induced VMT in a single surfactant system. The cleavage of intermolecular hydrogen bonds among the surfactant monomers seems to be the driving force for the salt-induced transition. The surfactant concentration-induced VMT is shown to be due to increase of pH of the surfactant solution. The vesicles are stable in the temperature range of 30−70 °C. The present study underlines the importance of hydrogen bonding on vesicle formation by this class of single-tailed surfactants. Furthermore, the introduction of the simple VMT system opens up the possibility of its use in various applications like controlled release. Work is going on in this laboratory in that direction.

**Acknowledgment.** This work was supported by the Department of Science and Technology (Grant No. SR/S1/PC-18/2005), New Delhi, India. AM thanks Central Instrumentation Facility, Birla Institute of Technology, Mesra, Ranchi, India for AFM and DLS measurements.

**Supporting Information Available:** The determination of *cac* using NPN probe, effect of temperature on stability of the vesicles, and $^1$H NMR spectra of the compound at two different concentrations. This material is available free of charge via the Internet at http://pubs.acs.org.

## References and Notes

(1) (a) Laughlin, R. G. *The aqueous phase behavior of surfactants*; Academic Press: London, 1994. (b) Evans, D. F.; Wennerstrom, H. *The Colloidal Domain*, Wiley-VCH: New York, 2001.

(2) (a) Fuhrhop, J. H.; Helfrich, W. *Chem. Rev.* **1993**, *93*, 1565. (b) Myers, D. *Surfaces, interfaces and Colloids: Principles and Applications*, Wiley-VCH: New York, 1991.

(3) (a) Yin, H.; Zhou, Z.; Huang, J.; Zheng, R.; Zhang, Y. *Angew. Chem. Int. Ed.* **2003**, *42*, 2188. (b) Yin, H.; Lei, S.; Zhu, S.; Huang, J.; Ye, J. *Chem. Eur. J* **2006**, *12*, 2825. (c) Hao, J. C.; Hoffmann, H.; Horbaschek, K. *J. Phys. Chem. B* **2000**, *104*, 10144. (d) Hassan, P. A.; Raghavan, S. R.; Kaler, E. W. *Langmuir* **2002**, *18*, 2543. (e) Mao, M.; Huang, J. B.; Zhu, B. Y.; Ye, J. P. *J. Phys. Chem. B* **2002**, *106*, 219. (f) Wang, C. Z.; Huang, J. B.; Tang, S. H.; Zhu, B. Y. *Langmuir* **2001**, *17*, 6389.

(4) Chen, W. J.; Zhai, L. M.; Li, G. Z.; Li, B. Q.; Xu, J. *J. Colloid Interface Sci*. **2004**, *278*, 447.

(5) (a) Davies, T. S.; Ketner, A. M.; Raghavan, S. R. *J. Am. Chem. Soc.* **2006**, *128*, 6669. (b) Hassan, P. A.; Valaulikar, B. S.; Manohar, C. F.; Bourdieu, K. L.; Candau, S. J. *Langmuir* **1996**, *12*, 4350. (c) Buwalda, R. T.; Stuart, M. C. A.; Engberts, J. *Langmuir* **2000**, *16*, 6780.

(6) (a) Yan, Y.; Hoffmann, H.; Drechsler, M.; Talmon, Y.; Makarsky, E. *J. Phys. Chem. B* **2006**, *110*, 5621. (b) Feitosa, E.; Bonassi, N. M.; Loh, W. *Langmuir* **2006**, *22*, 4512.

(7) (a) Zheng, Y.; Lin, Z.; Zakin, J. L.; Talmon, Y.; Davis, H. T.; Scriven, L. E. *J. Phys. Chem. B* **2000**, *104*, 5263. (b) Mendes, E.; Oda, R.; Manohar, C.; Narayanan, J. *J. Phys. Chem. B* **1998**, *102*, 338. (c) Mendes, E.; Narayanan, J.; Oda, R.; Kern, F.; Candau, S. J.; Manohar, C. *J. Phys. Chem. B* **1997**, *101*, 2256.

(8) Johnsson, M.; Wagenaar, A.; Engberts, J. B. F. N. *J. Am. Chem. Soc.* **2003**, *125*, 757.

(9) Grillo, I.; Kats, E. I.; Muratov, A. R. *Langmuir* **2003**, *19*, 4573.

(10) (a) Zhai, L.; Zhao, M.; Sun, D.; Hao, J.; Zhang, L. *J. Phys. Chem. B* **2005**, *109*, 5627. (b) Robinson, B. H.; Bucak, S.; Fontana, A. *Langmuir* **2000**, *16*, 8231.

(11) Lu, T.; Han, F.; Li, Z.; Huang, J.; Fu, H. *Langmuir* **2006**, *22*, 2045.

(12) (a) Mohanty, A.; Dey, J. *Chem. Commun.* **2003**, *12*, 1384. (b) Mohanty, A.; Dey, J. *J. Chromatogr A* **2005**, *1070*, 185. (c) Mohanty, A.; Dey, J. *J. Chromatogr A* **2006**, *1128*, 259.

(13) Mohanty, A.; Dey, J. *Talanta* **2007**, *71*, 1211.

(14) Mohanty, A.; Dey, J. *Langmuir* **2004**, *20*, 8452.

(15) Mohanty, A.; Dey, J. *Langmuir* **2007**, *23*, 1033.

(16) (a) Roy, S.; Mohanty, A.; Dey, J. *Chem. Phys. Lett.* **2005**, *414*, 23. (b) Prendergast, F. G.; Haugland, R. P.; Callahan, P. J. *Biochemistry* **1981**, *20*, 7333. (c) Lentz, B. R. *Chem. Phys. Lipids* **1993**, *64*, 99. (d) Shinitzky, M.; Yuli, I. *Chem. Phys. Lipids* **1982**, *30*, 261.

(17) (a) Hoffmann, H. In *Structure and Flow in Surfactant Solutions*; C. Herb, R. K. Prud'homme Eds.; American Chemical Society: Washington DC, 1994; pp 2−31. (b) Cates, M. E.; Candau, S. J. *J. Phys.: Condens. Matter* **1990**, *2*, 6869.

(18) Khatua, D.; Dey, J. *J. Phys. Chem. B* **2007**, *111*, 124.

(19) (a) Roy, S.; Dey, J. *Langmuir* **2003**, *19*, 9625. (b) Roy, S.; Dey, J. *Langmuir* **2005**, *21*, 10362.

(20) Gonazalez, Y. I.; Nakanishi, H.; Stjerndahl, M.; Kaler, E.W. *J. Phys. Chem. B* **2005**, *109*, 11675 and references therein.

(21) (a) Chandra, A. *Phys. Rev. Lett.* **2000**, *85*, 768. (b) Smith, J. S.; Scholtz, J. M. *Biochemistry* **1998**, *37*, 33. (c) Hassan, S. A. *J. Phys. Chem. B* **2005**, *109*, 21989.

(22) Pandit, S. A.; Berkowitz, M. L. *Biophys. J* **2002**, *82*, 1818.